

Example of Geohazard Map using Digital Elevation Model (DEM) data

A 10-m digital elevation model (DEM) data layer was used to calculate hillshade depictions at three different illumination angles to allow interpretation of landforms associated with landslides and debris flows. Illumination from northwest (315 azimuth), northeast (045 azimuth), and south (180 azimuth) at inclination of 35° above the local horizon are depicted in Figure 1. Slope and aspect results are displayed, along with roughness calculated for the center of a moving 9x9 array.

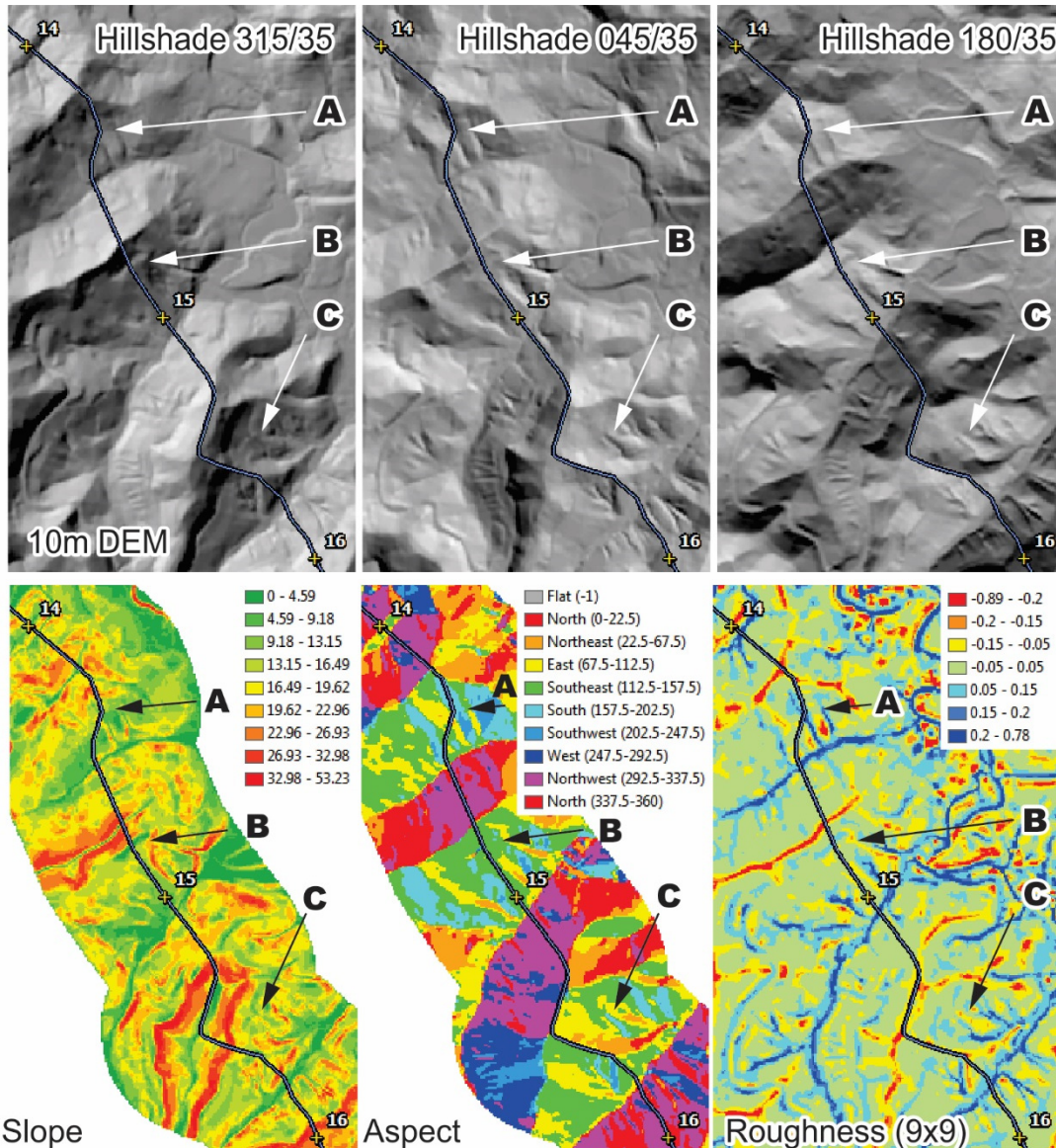


Figure 1. Calculated GIS layers for a two-mile stretch of pipeline alignment in West Virginia. Hillshade, slope, and aspect are GIS utilities; roughness was calculated for the center of a moving array of 81 pixels (9x9) using  $rg_h = (\text{array\_mean} - \text{DEM}) / \text{array\_range}$

Three points (A, B, and C) are identified in Figure 1 to illustrate geohazard interpretation. Point A is a right-hand bend at about MP 14.4, Point B is a topographic bench at about MP 14.8, and Point C is irregular terrain at about MP 15.6. Point A was identified because the right-hand bend (PI) is located in a first-order stream channel, the head of which ends at a steep spot. Such topographic features are called ‘hillslope hollows’ or swales and are known to be debris flow source areas (Keaton et al., 1985). The hollow and the channel below it tend to have higher soil moisture than adjacent slopes and ridges. Construction activities on this slope would need to be done to minimize the potential for destabilizing the channel and slope. The roughness panel in Figure 1 make the channel stand out with blue color that represents concave slope elements; by contrast, the red color in the roughness panel represents convex slope elements that are ridges.

Point B in Figure 1 represents a bench that is visible in the hillshade, slope, and roughness panels. The contour-like feature in the hillshade panels suggests that this is a road; in this geology such a feature may be a coal seam that has been exposed for small-scale mining. The bench would represent the deposits of excavated earth materials. The pipeline trench across the bench would be in ‘fill’ deposits and might be less stable than slopes without benches.

Point C refers to irregular terrain that appears to be a landslide deposit. The pipeline alignment at this location appears to be on a narrow secondary ridge with landslide deposits on both sides. The roughness panel in Figure 1 shows some concave elements in light blue color on both sides of the pipeline alignment, and a first-order channel ending in a hillslope hollow on the right side of the alignment adjacent to a small-angle right-hand bend.

Landslide inventory maps, by their nature, tend to overlook apparently stable, non-landslide terrain, and, as can be seen in the hillshade panels in Figure 1, different illumination angles allow landslide features to stand out or be subdued. Landslide inventory mapping could be improved if regional comprehensive landslide hazard evaluations produced probability distributions (Keaton and Haneberg, 2013); however, a comprehensive landslide hazard evaluation has not been compiled for the Appalachian Mountains.

Landslides are secondary events triggered by a primary event or process, such as precipitation or earthquakes. Hurricane-induced torrential storms have occurred in the Appalachian Mountains and produced landslides and debris flows (Wieczorek and Morgan, 2008). Therefore, the annual frequency of landslides or debris flows depends on the annual frequency of triggering events, and landslides and debris flows do not always happen at every susceptible location when triggering events occur (Keaton and Roth, 2008). For a risk analysis, probability distributions developed for one of the few localities where they are available could be used with the understanding that no specific evaluation has been prepared for the Appalachian Mountains. An approach that is available now is to map apparently stable slopes and landslides with comparable level of detail (Keaton and Rinne, 2002; Keaton and Roth, 2015). This approach differentiates five classes of slope and landslides: 1) unstable slopes, 2) slopes with inactive landslides, 3) potentially unstable slopes, 4) apparently stable landslides, and 5) apparently stable slopes. Such an approach would be helpful for a quantitative risk analysis of geohazards.

Ground subsidence and settlement can be related to sinkhole activity (karst) in areas underlain by soluble bedrock or soil formations, or caused by groundwater pumping in unconsolidated formation.

Amec Foster Wheeler has the capability to acquire synthetic aperture radar (SAR) satellite data and process it for interpretation of regional ground subsidence, as we did recently at a site in south-central Mississippi (Panda et al., 2015).

The distribution of soluble bedrock and soil formations has been compiled by the U.S. Geological Survey; the pipeline alignment crosses sinkhole-prone terrain in West Virginia and Virginia and comes close to it in North Carolina. Calculated GIS products in Figure 2 reveal several sinkholes in an area underlain by two dolostone formations. The GIS panels in Figure 2 are similar to those in Figure 1, except the base DEM in Figure 2 has a pixel dimension of 3 m instead of 10-m.

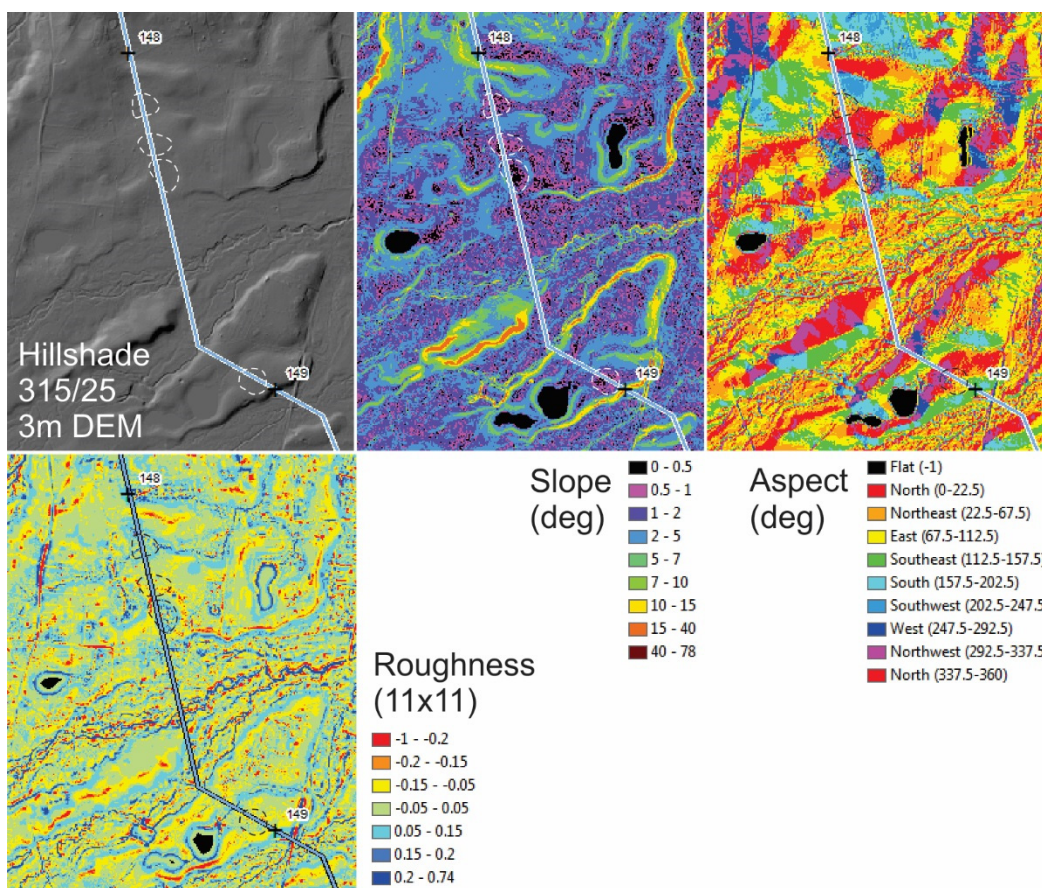


Figure 2. Calculated GIS layers for a one-mile stretch of the ACP alignment in Virginia. Hillshade, slope, and aspect are GIS utilities; roughness was calculated for the center of a moving array of 121 pixels (11x11) using  $rg_h = (\text{array\_mean} - \text{DEM}) / \text{array\_range}$ .

Oval depressions are apparent in the hillshade panel in Figure 2, and can be identified in the slope, aspect, and roughness panels, also. Fine dashed white lines were used to trace areas in the slope panel along the pipeline alignment that has characteristics similar to the features that are most likely sinkholes. The dashed lines from the slope panel were copied onto the aspect and roughness panels as black lines, and the hillshade panel as dashed white lines. Thus, it appears that four potential

sinkhole areas are located along the pipeline alignment between MP 148 and MP 149. The river channel between about MP 148.5 and MP 148.8 could be concealing other potential sinkholes that do not have surface expression. This portion of the alignment could be evaluated with geophysical methods, such as electrical resistivity or micro gravity. Ground penetrating radar has been successful in detecting subsurface voids in some locations; however, it does not work well in clay-rich or saturated soils.

Sinkhole occurrence has not been documented systematically in the United States. Florida established a database of reported sinkholes that is maintained by the Florida Geological Survey. The events included in this database have not been verified and the date associated with the entry is the date of reporting, not necessarily the date of occurrence. Nonetheless, the Florida sinkhole incident report database is the best available and was used by Keaton and Boudra (2014) for characterizing sinkhole hazard for pipeline risk assessment in Florida and could be modified for use elsewhere.

### **Technical References**

Keaton, J.R., Anderson, L.R., and Brooks, R.K., 1985, Geomorphology, geometry, and evidence for recurrence of slope failures in steep swales in metamorphic rock filled with colluvial and residual debris in the Wasatch Range near Farmington, Utah (abstract): *Eos*, v. 66, no. 46, November 15, p. 900.

Keaton, J.R., and Boudra, L.H., 2014, Development of Sinkhole Hazard for Pipeline Risk Assessment in Northern Florida, in *Proceedings of the 10th International Pipeline Conference*, Sept 29-Oct 3, 2014, Calgary, Alberta, Canada, in review IPC2014-33117, 6 p.

Keaton, J.R. and Haneberg, W.C., 2013, Landslide inventories and uncertainty associated with ground truth, in F. Wu and S. Qi, editors, *Global View of Engineering Geology and the Environment*. London, Taylor & Francis, p. 105-110.

Keaton, J.R., and Rinne, R., 2002, Engineering-geology mapping of slopes and landslides, in Bobrowsky, P.T., ed., *Geoenvironmental Mapping, Methods, Theory and Practice*: Rotterdam, Balkema, p. 9-27.

Keaton, J.R., and Roth, R.J., Jr., 2008, Mapping Landslides for the Insurance Industry – Lessons from Earthquakes: *Proceedings, EUROENGE02008 Madrid, Spain, II European Conference of International Association for Engineering Geology*, CD Paper 063, 6 p.

Keaton, J.R., and Roth, R.J., Jr., 2015, Defining Areas with Nil Landslide Hazard is a step toward a Comprehensive Landslide Loss Model: *Association of Environmental and Engineering Geologists Professional Forum on Landslides*, Seattle, February 26-27.

Panda, B., Keaton, J. and Ruggeri, R., 2015, InSAR Evaluation of Ground Heave and Subsidence near an Underground Gas Storage Facility: *Fringe 2015 Workshop Advances in the Science and Applications of SAR Interferometry and Sentinel-1 InSAR Workshop*, European Space Agency, Rome, March 23-27, 2015.

Wieczorek, G.F., and Morgan, B.A., 2008, Debris-Flow Hazards within the Appalachian Mountains of the Eastern United States: *U.S. Geological Survey Fact Sheet 2008-3070*.